AIP | Physics of Plasmas

Effect of the inductive electric field on ion flow in tokamaks

Peter J. Catto, R. J. Hastie, I. H. Hutchinson, and P. Helander

Citation: Phys. Plasmas 8, 3334 (2001); doi: 10.1063/1.1373676
View online: http://dx.doi.org/10.1063/1.1373676
View Table of Contents: http://pop.aip.org/resource/1/PHPAEN/v8/i7
Published by the American Institute of Physics.

Effect of the inductive electric field on ion flow in tokamaks

Peter J. Catto, R. J. Hastie, and I. H. Hutchinson
Massachusetts Institute of Technology, Plasma Science and Fusion Center, Cambridge, Massachusetts 02139

P. Helander
EURATOM/UKAEA Fusion Association, Culham Science Centre, Abingdon OX14 3DB, United Kingdom

(Received 6 December 2000; accepted 15 January 2001)

The effect of the inductive electric field of a tokamak on the parallel (and poloidal) ion flow in the banana regime is evaluated. It is demonstrated that the flow is in the direction of the parallel current and is surprisingly large—comparable to the usual banana regime ion temperature gradient drive.
 [DOI: 10.1063/1.1373676]

I. INTRODUCTION

Recent observations of strong toroidal ion flows in Alcator C-Mod during Ohmic operation[1] have motivated us to consider the effect of the inductive electric field in a tokamak on the parallel and poloidal flow of ions. Typically the observed toroidal flows are about a tenth or less of the ion thermal speed and are in the direction of the plasma current (that is, co-directed) for high confinement (H-mode) operation. In neoclassical theory the influence of the inductive parallel electric field on ion transport is invariably ignored. This neglect decouples the ions from the electrons and is normally referred to as the ''weak coupling approximation.''[2] Because the role of the inductive electric field on ion transport is expected to be weak, its impact on ion flow in tokamaks has been assumed to be insignificant as well. However, in what follows we will demonstrate that this is not the case. Indeed, we will show that in the banana regime the inductive electric field can drive parallel and poloidal ion flow comparable to the usual ion temperature gradient flow of neoclassical theory.[2,3] It is important to remember, however, that the inductive electric field is not a source of toroidal momentum in a quasi-neutral plasma since it does not explicitly enter the total conservation of toroidal angular momentum equation which determines the radial electric field. Therefore, any inductively driven toroidal flow acts to alter the relation between the radial electric field and toroidal rotation and is not a complete explanation of the Alcator C-Mod observations.

In a plasma with no parallel variation of the magnetic-field strength, for example, a straight circular cylinder with helical field, the parallel electric field, $E_{\parallel}$, does not impose any ion flow constraint because the electric field force acting on the ions is exactly balanced by the collisional friction with the electrons. The parallel ion flow is then indeterminate in this classical case; it is not connected with $E_{\parallel}$.

Neoclassically, however, in a magnetic-field configuration such as a tokamak, with field magnitude variation, the parallel electric field force on the trapped electrons is balanced not by friction, but by the mirror force. The consequence of this mirror force is the Ware–Galeev trapped particle pinch,[4,5] and, of course, the neoclassical reduction in conductivity.[2,3] The passing electrons have their electric field force balanced by collisional friction. We denote the fraction of the parallel electric field force on the total electron population that is balanced by friction with the ions as I: The effective passing fraction. The ions, therefore, experience an average parallel force per unit charge $E_{*} \sim E_{\parallel}(1-I)$ consisting of the difference between the direct electric field force, $E_{\parallel}$, and the electron friction, $E_{\parallel}I$. In equilibrium the total force E_{*} on both the trapping and passing ions must be balanced by the mirror force on the trapped ions, and when it is, the Ware–Galeev pinch of the ions will exactly equal that on the electrons, maintaining ambipolarity. The passing ions transfer the force E_{*} to the trapped ions by collisions and they balance it with the mirror force. In order that the mirror force on the ions has its correct value, the ions must adopt a flow with a specific mean parallel velocity $V_{\parallel i}$. A rough estimate of its magnitude may be obtained as follows.

The passing ions (mass M, charge Ze, and mean velocity V_p) transfer their momentum per particle MV_p to the stationary trapped ions at a rate of approximately $(1-I)\nu_{ii}$, where ν_{ii} is the ion–ion collision frequency and the trapped ion fraction is taken as $1-I$. Therefore, the drag force per unit charge on the passing ions is $MV_p(1-I)\nu_{ii}/Ze$. Setting this equal to E_{*}, and noting that the average parallel ion velocity, $V_{\parallel i}$, is related to V_p by $V_{\parallel i} \sim IV_p$ gives $MV_{\parallel i}(1-I)\nu_{ii} \sim ZeE_{\parallel}I(1-I)$. Notice that the parallel ion flow $V_{\parallel i}$ is co-directed and that in the absence of trapped particles $(I=1)$ is undetermined. Rewriting for $I \neq 1$, we obtain the parallel ion flow estimate

$$V_{\parallel i} - ZeE_{\parallel}I/M\nu_{ii}.$$

Of course the coefficients in this equation based on a heuristic derivation are not quantitatively reliable. The purpose of the present work is to perform a full kinetic theory calculation of this effect and to show that its magnitude is significant.

In Sec. II we solve a model ion kinetic equation[6,7] to evaluate the effect on the ions of an unbalanced parallel electric field and parallel friction between the ions and electrons. More sophisticated ion–ion collision operators[8] giving slightly different numerical factors are considered in Appendix A. Section III solves a model electron kinetic equation to determine the relation between the parallel electric field and the ion–electron friction and demonstrates that this relation is related to the usual inward Ware–Galeev trapped particle pinch. At first only ion charge numbers much greater than unity ($Z \gg 1$) are considered in Sec. III for simplicity. However, the result for large aspect ratio and general Z is then obtained from standard neoclassical results and Appendix B considers arbitrary aspect ratio and Z. The parallel and poloidal ion flow is evaluated in Sec. IV and we conclude with a discussion in the last section.

II. ION KINETIC EQUATION AND SOLUTION

To focus on the inductive electric field effects on the ions we ignore the usual ion temperature drive of standard neoclassical theory and solve for the ion response by considering the reduced linearized ion kinetic equation[2,3]

$$v_\parallel \mathbf{n}\cdot\nabla f_{1i} - C_{ii}\{f_{1i}\} = \frac{Ze}{T_i} E_* v_\parallel f_{0i}, \tag{1}$$

where f_{1j} is the perturbed distribution function of species j and C_{ii} is the linearized ion–ion collision operator. The ion charge is $Ze, \mathbf{n}=\mathbf{B}/B$ is the unit vector along the magnetic-field $\mathbf{B}$, the parallel velocity is $v_\parallel = (v^2 - 2\mu B)^{1/2}$ with v the speed, and the gradient is taken with the magnetic moment $\mu = v_\perp^2/2B$ held fixed. The quantity E_* is defined as

$$E_* = E_\parallel - \frac{F_{\parallel ei}}{eN_e}, \tag{2}$$

with $E_\parallel$ the parallel electric field, and the parallel friction between the electrons and ions is defined by

$$F_{\parallel ei} = m\int d^3v\, v_\parallel C_{ei}\{f_{1e}\}. \tag{3}$$

The unperturbed ion distribution function f_{0i} is Maxwellian

$$f_{0i} = N_i\left(\frac{M}{2\pi T_i}\right)^{3/2} \exp\left(-\frac{Mv^2}{2T_i}\right), \tag{4}$$

with N_i and T_i the ion density and temperature, and M the ion mass. The electron density is N_e and m is the electron mass, and quasineutrality requires $N_e = ZN_i$.

In the banana regime $\mathbf{n}\cdot\nabla f_{1i}=0$ to lowest order. To next order we annihilate the streaming term by multiplying by $B/(v_\parallel \mathbf{B}\cdot\nabla\vartheta)$ with ϑ the poloidal angle, and integrating over a full poloidal circuit (a full bounce for the trapped and 2π for the passing). Defining $d\tau = d\vartheta B/v_\parallel \mathbf{B}\cdot\nabla\vartheta$ as the incremental time along the trajectory, the resulting constraint equation to be solved becomes

$$\oint d\tau C_{ii}\{f_{1i}\} = -\frac{Ze}{T_i} f_{0i} \oint d\tau v_\parallel E_*. \tag{5}$$

For the trapped (subscript t) ions $\oint d\tau v_\parallel E_* = 0$, while C_{ii} is even in $v_\parallel$ so that

$$f_{1i}|_t = 0. \tag{6}$$

For the passing (subscript p) the orbit average is equivalent to a flux surface average and Eq. (5) may be rewritten as

$$\left\langle \frac{B}{v_\parallel} C_{ii}\{f_{1i}|_p\}\right\rangle = -\frac{Ze}{T_i} f_{0i}\langle BE_*\rangle, \tag{7}$$

where $\langle\cdots\rangle = [\int_{-\pi}^{\pi} d\vartheta(\cdots)/\mathbf{B}\cdot\nabla\vartheta]/[\int_{-\pi}^{\pi} d\vartheta/\mathbf{B}\cdot\nabla\vartheta]$. Notice that in the banana regime the solution for f_{1i} is odd in $v_\parallel$, while its next order correction in collision over transit frequency is even in $v_\parallel$. The $Bv_\parallel$ moment and flux surface average of Eq. (1)

$$eN_e\langle BE_*\rangle = -M\left\langle \int d^3v\, f_{1i} v_\parallel \mathbf{n}\cdot\nabla(v_\parallel B)\right\rangle,$$

places a constraint on this next order even solution.

To illustrate the solution of Eq. (7) we consider the Kovrizhnikh model like–particle collision operator, which retains pitch angle scattering and conserves momentum as well as energy and number [see Appendix A of Ref. 6 or Ref. 7, for example]; namely

$$C_{jj}\{f_{1j}\} = \nu v_\parallel\left[\frac{\partial}{\partial\mu}\left(\frac{\mu v_\parallel}{B}\frac{\partial f_{1j}}{\partial\mu}\right) + \frac{f_{0j}\int d^3v\, \nu v_\parallel f_{1j}}{\int d^3v\, \nu v_\parallel^2 f_{0j}}\right], \tag{8}$$

where

$$\nu = \nu_{jj} Q(x) = \frac{\nu_{jj}}{x^3}\left[\left(1-\frac{1}{2x^2}\right)Erf(x) + \frac{Erf'(x)}{2x}\right], \tag{9}$$

$Erf(x) = 2\pi^{-1/2}\int_0^x dt \exp(-t^2)$ is the error function, $Erf'(x) = dErf(x)/dx$, and for ions $x=(Mv^2/2T_i)^{1/2}$ and $\nu_{ii} = 2^{1/2}\pi Z^4 e^4 N_i \ln\Lambda/M^{1/2} T_i^{3/2}$ with $\ln\Lambda$ the Coulomb logarithm.

Employing Eq. (8) and defining

$$Y = \langle B\int d^3v\, \nu v_\parallel f_{1i}\rangle \tag{10}$$

and

$$W = -\frac{Ze}{T_i \nu}\langle BE_*\rangle - \frac{Y}{\int d^3v\, \nu v_\parallel^2 f_{0i}}, \tag{11}$$

Eq. (7) becomes

$$\frac{\partial}{\partial\mu}\left(\mu\langle v_\parallel\rangle \frac{\partial f_{1i}|_p}{\partial\mu}\right) = W f_{0i}. \tag{12}$$

Integrating from $\mu=0$ to μ gives

$$\frac{\partial f_{1i}|_p}{\partial\mu} = \frac{W f_{0i}}{\langle v_\parallel\rangle}. \tag{13}$$

Using Eqs. (6) and (13) to evaluate Y gives

$$(1-I)Y = -\frac{ZeN_i}{M}\langle BE_*\rangle I, \tag{14}$$

where the effective fraction of passing particles[3] is

$$I = \frac{3}{4}\langle B^2\rangle \int_0^{B_{\max}^{-1}} \frac{d\lambda\,\lambda}{\langle(1-\lambda B)^{1/2}\rangle} \approx 1 - 1.46\varepsilon^{1/2} + \cdots, \tag{15}$$

with $R/R_0 = B_0/B = 1+\varepsilon\cos\vartheta$, $\lambda = 2\mu/v^2$ a pitch angle variable, and $\varepsilon = r/R_0$ the inverse aspect ratio. The expression on the far right-hand side of (15) is the lowest order result for circular flux surfaces and large aspect ratio; the integral form is valid for general geometry. In the next section we will show that $E_*=0$ in the cylindrical limit $\varepsilon=0$, so that in this limit Y is unconstrained by Eq. (14). As a

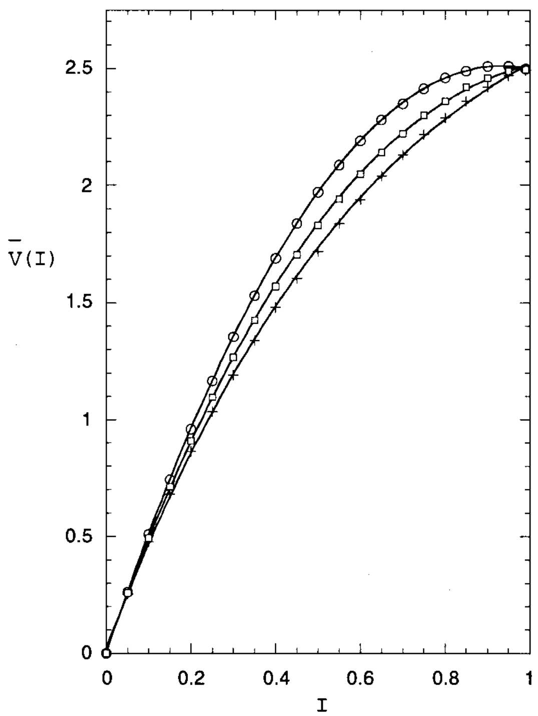

FIG. 1. Plots of $\overline{V}$ as defined in Eq. (20) vs I for the three different model ion–ion collision operators. Equation (18) results are shown as the upper curve, the full Hirshman–Sigmar operator gives the lower curve, and the middle curve is obtained from the lowest order Hirshman–Sigmar operator.

result, Y is free to adjust to conserve parallel momentum when the cylindrical limit of Eqs. (7) and (8) is considered.

Using Eq. (14) we can evaluate Eq. (11) and thereby rewrite Eq. (13) as

$$\frac{\partial f_{1i}|_p}{\partial \mu} = -\frac{Ze}{T_i \nu}\left[1 + \frac{N_i T_i I \nu}{(1-I)M\int d^3v\, \nu v_\parallel^2 f_{0i}}\right]\frac{\langle BE_*\rangle}{\langle v_\parallel\rangle}. \quad (16)$$

Equation (16) can then be used to evaluate the parallel ion flow

$$N_i V_{\parallel i} = \int d^3v\, v_\parallel f_{1i}, \quad (17)$$

to find

$$V_{\parallel i} = \frac{ZeB\langle BE_*\rangle I}{M\langle B^2\rangle \nu_{ii}}\left[\frac{I}{(1-I)\langle\langle Q\rangle\rangle} + \left\langle\left\langle \frac{1}{Q}\right\rangle\right\rangle\right], \quad (18)$$

where we define

$$\langle\langle Q^q\rangle\rangle = \frac{\int_0^\infty dx\, Q^q x^4 \exp(-x^2)}{\int_0^\infty dx\, x^4 \exp(-x^2)}, \quad (19)$$

and, upon evaluating, obtain the coefficients $\langle\langle Q\rangle\rangle = 0.4$ and $\langle\langle Q^{-1}\rangle\rangle = 5.4$. Of course, the coefficients $\langle\langle Q\rangle\rangle$ and $\langle\langle Q^{-1}\rangle\rangle$ are sensitive to the details of the model ion–ion collision operator employed. In Appendix A the more sophisticated model collision operators of Hirshman and Sigmar[8] are used to obtain the same result to within about 10% as shown in Fig. 1, which plots

$$\overline{V} \equiv \frac{M\nu_{ii}\langle B^2\rangle V_{\parallel i}}{ZeB\langle BE_*\rangle I}, \quad (20)$$

versus I. In Fig. 1, Eq. (18) results in the upper curve, the full Hirshman–Sigmar operator gives the lower curve, and the middle curve is obtained from the lowest order Hirshman–Sigmar operator.

III. ELECTRON KINETIC EQUATION AND SOLUTION

To determine the relation between the parallel electric field and the electron–ion friction, that is, E_*, the electron kinetic equation must be solved. Again, we keep only the inductive parallel electric field as the drive so we need only consider

$$v_\parallel \mathbf{n}\cdot\nabla f_{1e} - C_{ei}\{f_{1e}\} - C_{ee}\{f_{1e}\} = -\frac{e}{T_e}E_\parallel v_\parallel f_{0e}, \quad (21)$$

where C_{ee} and C_{ei} are the electron–electron and electron–ion collision operators, and f_{0e} is a Maxwellian with T_e the electron temperature

$$f_{0e} = N_e\left(\frac{m}{2\pi T_e}\right)^{3/2}\exp\left(-\frac{mv^2}{2T_e}\right).$$

To solve Eq. (21) and evaluate the parallel electron–ion friction from Eq. (3) it is convenient to introduce the Spitzer function f_{1s} which is the solution of[2,9]

$$L_{ei}\{f_{1s}\} + C_{ee}\{f_{1s}\} = \frac{e}{T_e}E_\parallel v_\parallel f_{0e}, \quad (22)$$

where L_{ei} is the Lorentz operator

$$L_{ei}\{h\} = \nu_{ei} v_\parallel \frac{\partial}{\partial\mu}\left(\frac{\mu v_\parallel}{B}\frac{\partial h}{\partial \mu}\right), \quad (23)$$

with $\nu_{ei} = \nu_{ee}Z/x^3$ and $\nu_{ee} = 2^{1/2}\pi e^4 N_e \ln\Lambda/m^{1/2}T_e^{3/2}$ for $ZN_i = N_e$, and $x = (mv^2/2T_e)^{1/2}$ for electrons. Using Eq. (22) and conservation of momentum in like particle collisions to rewrite Eq. (3), gives

$$F_{\parallel ei} = eN_e E_\parallel + m\int d^3v\, v_\parallel L_{ei}\{f_{1e} - f_{1s} - mV_{\parallel i} v_\parallel f_{0e}/T_e\}, \quad (24)$$

where we make use of

$$C_{ei}\{f_{1e}\} = L_{ei}\{f_{1e} - mV_{\parallel i} v_\parallel f_{0e}/T_e\}. \quad (25)$$

From this form we see that the $V_{\parallel i}$ term in the Lorentz operator is negligible since it will result in corrections to Eq. (18) on the order of $(m/M)^{1/2}$. Interestingly, the $V_{\parallel i}$ correction in Eq. (25) and the usual pressure and temperature gradient terms, which are of the same order, are responsible for the weak coupling corrections to the heat and particle fluxes estimated in Table IV of Ref. 2. However, the modification of the parallel ion flow due to the inductive electric field is not considered there.

To determine f_{1e} we must solve the electron kinetic equation (written in terms of the Spitzer function)

$$v_\parallel \mathbf{n}\cdot\nabla f_{1e} = L_{ei}\{f_{1e} - f_{1s}\} + C_{ee}\{f_{1e} - f_{1s}\}. \quad (26)$$

In the banana limit $\mathbf{n}\cdot\nabla f_{1e}=0$ to lowest order, while annihilating the streaming term to next order gives the constraint equation

$$\oint d\tau[L_{ei}\{f_{1e}-f_{1s}\}+C_{ee}\{f_{1e}-f_{1s}\}]=0, \tag{27}$$

where, as in Eq. (5), the time integral is over the closed periodic motion. For the trapped electrons $\oint d\tau L_{ei}\{f_{1s}\}=0=\oint C_{ee}\{f_{1s}\}$ giving

$$f_{1e}|_t=0. \tag{28}$$

To illustrate simply the evaluation of E_* we consider the $Z \gg 1$ limit so electron–electron collisions can be ignored in evaluating the passing electron response. As a result, the Spitzer function is simply

$$f_{1s}=-\frac{eE_\parallel v_\parallel f_{0e}}{T_e\nu_{ei}}, \tag{29}$$

and the passing electron constraint becomes

$$\frac{\partial}{\partial\mu}\left(\mu\langle v_\parallel\rangle\frac{\partial f_{1e}|_p}{\partial\mu}-\mu\left\langle v_\parallel\frac{\partial f_{1s}}{\partial\mu}\right\rangle\right)=0. \tag{30}$$

Integrating Eq. (30) from $\mu=0$ to μ and inserting Eq. (29) gives the passing electron response

$$\frac{\partial f_{1e}|_p}{\partial\mu}=\frac{\langle v_\parallel\partial f_{1s}/\partial\mu\rangle}{\langle v_\parallel\rangle}=\frac{e\langle BE_\parallel\rangle f_{0e}}{T_e\nu_{ei}\langle v_\parallel\rangle}. \tag{31}$$

Inserting Eqs. (28), (29), and (31) into Eq. (24), performing the integrals, and multiplying by B and flux surface averaging gives

$$\langle BE_*\rangle=(1-1)\langle BE_\parallel\rangle, \tag{32}$$

where I is defined as in Eq. (15). Notice that $E_*=0$ for $\varepsilon=0$ so that the parallel electric field and parallel electron–ion friction balance in a cylinder as required. Moreover, the solution for f_{1e} is odd in $v_\parallel$, while its next order in collision over transit frequency correction is even in $v_\parallel$ and must satisfy the constraint placed on it by $Bv_\parallel$ moment and flux surface average of Eq. (26)

$$eN_e\langle BE_*\rangle=m\langle\int d^3v f_{1e}v_\parallel\mathbf{n}\cdot\nabla(v_\parallel B)\rangle.$$

The result (32) can be obtained for large aspect ratio by considering the moment expression for the particle flux Γ obtained by forming the $mcRB_Tv_\parallel/eB$ moment of Eq. (25)

$$\begin{aligned}\Gamma&\equiv\int d^3v f_{1e}RB_Tv_\parallel\cdot\nabla(mcv_\parallel/eB)\\&=\int d^3v f_{1e}\mathbf{v}_d\cdot\nabla\psi\\&=-cN_eRB_T\langle E_*/B\rangle\approx-cN_eRB_T\langle BE_*\rangle/\langle B^2\rangle,\end{aligned} \tag{33}$$

where $\mathbf{v}_d$ is the curvature plus ∇B drift velocity, B_T is the toroidal magnetic field, and higher order terms in ε have been neglected in the expression on the far right-hand side. Standard high aspect ratio banana regime transport theory for $Z\gg1$ in the absence of pressure and temperature gradients finds[2]

$$\Gamma\approx-1.46\varepsilon^{1/2}cN_eRB_T\langle BE_*\rangle/\langle B^2\rangle, \tag{34}$$

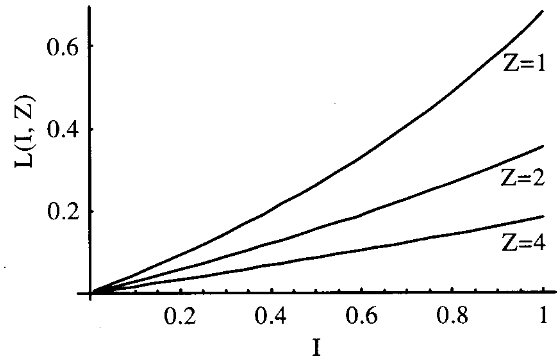

FIG. 2. The enhancement factor L in Eq. (35) due to electron–electron collisions plotted vs I for $Z=1$, 2, and 4 for the model operator of Eq. (8).

which when combined with Eq. (33) is consistent with Eq. (32). Consequently, the relation between the parallel electric field and the parallel friction is contained in the standard large aspect ratio banana regime results.

The evaluation of $\langle BE_*\rangle$ is repeated in Appendix B keeping electron–electron collisions with the model operator of Eqs. (8) and (9) to find

$$\begin{aligned}\langle BE_*\rangle&=(1-I)\langle BE_\parallel\rangle\left[1+\frac{I\langle\langle Q\rangle\rangle\langle\langle Q_Z\rangle\rangle}{\langle\langle Q\rangle\rangle-I\langle\langle QQ_Z\rangle\rangle}\right]\\&\equiv(1-I)\langle BE_\parallel\rangle[1+L(I,Z)],\end{aligned} \tag{35}$$

where $Q=Q(x)$ is as defined in Eq. (9) but with $x=(mv^2/2T_e)^{1/2}$, and $Q_Z=Q/[Q+(Z/x^3)]$. The function L is positive since $\langle\langle Q\rangle\rangle-I\langle\langle QQ_Z\rangle\rangle=\langle\langle Q_ZZ/x^3\rangle\rangle+(1-I)\times\langle\langle QQ_Z\rangle\rangle$ and depends only on I and Z. It represents the enhancement due to electron–electron collisions and is plotted versus I for $Z=1$, 2, and 4 in Fig. 2. The I dependence is explicit in L, and the Z dependence of $\langle\langle Q_Z\rangle\rangle$ can be fitted to find the approximate expression

$$L(I,Z)=\frac{0.68(Z-0.38)I}{Z^2-(0.55Z-0.18)I}. \tag{36}$$

Repeating the alternative banana regime derivation of Eqs. (33) and (34) with the variationally determined transport coefficients for arbitrary Z and large aspect ratio[2] gives the relation between $\langle BE_*\rangle$ and $\langle BE_\parallel\rangle$ to be

$$\langle BE_*\rangle=1.46[1+(0.67/Z)]\varepsilon^{1/2}\langle BE_\parallel\rangle. \tag{37}$$

In this limit electron–electron collisions enhance the ion flow by the factor $[1+(0.67/Z)]$, which agrees with Eq. (36) for $Z=1$ and ∞; the slight disagreements at intermediate Z are because of our use of a model like particle collision operator to obtain Eq. (35).

IV. PARALLEL AND POLOIDAL ION FLOW

To determine the parallel ion flow we need only insert Eq. (33) into Eq. (18)

$$V_{\parallel i}=\frac{ZeB\langle BE_{\parallel}\rangle(1+L)I}{M\nu_{ii}\langle B^2\rangle}\left[\frac{1}{\langle\langle Q\rangle\rangle}+(1-I)\left\langle\left\langle\frac{1}{Q}\right\rangle\right\rangle\right]. \tag{38}$$

The ion–ion collision frequency in Eq. (38) and elsewhere is $3(2\pi)^{1/2}/(4\tau_i)$, where τ_i is the Braginskii collision time. As noted earlier, the $\langle\langle Q^p\rangle\rangle$ and L coefficients in Eq. (38) are sensitive to the details of the like particle collision model employed, and L depends on I and Z as well. Based on the results in Appendix A and Fig. 1, errors of about 10% are expected.

To compare the parallel ion flow to the ion thermal speed $v_i=(2T_i/M)^{1/2}$ we first define the loop voltage $V_{\rm loop}=2\pi RE_{\parallel}$ and ion mean free path $\lambda_i=v_i/\nu_{ii}$. Then for $Z=1$ and keeping $\varepsilon^{1/2}$ corrections, Eq. (38) can be used to estimate

$$\frac{V_{\parallel i}}{v_i}\approx 4.2(1-0.7\varepsilon^{1/2})\frac{\lambda_i eV_{\rm loop}}{2\pi RT_i}, \tag{39}$$

where $I=1-1.46\varepsilon^{1/2}$, $1+L=1.67(1-0.9\varepsilon^{1/2})$, $\langle\langle Q\rangle\rangle=0.4$, and $(1-I)\langle\langle Q^{-1}\rangle\rangle=7.9\varepsilon^{1/2}$ are employed. For Alcator C-Mod parameters of $R=70\,\rm cm$, $\varepsilon=10^{-1}$, $V_{\rm loop}=1$ volt, $N_e=2\times10^{14}\,\rm cm^{-3}$, and $T_i=1\,\rm keV$, we find $V_{\parallel i}/v_i\sim3\times10^{-2}$; reasonably close to the magnitude of the flows observed in C-Mod.[1]

The flow we have calculated should be added to the usual neoclassical expression for the parallel velocity[2,10] to obtain

$$V_{\parallel i}\big|_{\rm tot}=\frac{cT_i}{eB_p}\left[1.17(1-0.67\varepsilon^{1/2})\frac{d\ln T_i}{dr}-\frac{d\ln p_i}{dr}-\frac{e}{T_i}\frac{d\Phi}{dr}\right]+\frac{eB\langle BE_{\parallel}\rangle(1+L)I}{M\nu_{ii}\langle B^2\rangle}\left[\frac{I}{\langle\langle Q\rangle\rangle}+(1-I)\left\langle\left\langle\frac{1}{Q}\right\rangle\right\rangle\right], \tag{40}$$

where B_p is the poloidal magnetic field and we have taken $Z=1$. In fact, our new term is an addition to the poloidal flow, normally represented by just the ion temperature gradient term, which now becomes

$$V_i\big|_{\rm pol}=\frac{1.17(1-0.67\varepsilon^{1/2})c}{eB}\frac{dT_i}{dr}+\frac{eB_p\langle BE_{\parallel}\rangle(1+L)I}{M\nu_{ii}\langle B^2\rangle}\times\left[\frac{I}{\langle\langle Q\rangle\rangle}+(1-I)\left\langle\left\langle\frac{1}{Q}\right\rangle\right\rangle\right]. \tag{41}$$

It is, therefore, perhaps of most interest to compare the inductive velocity with that caused by ion temperature gradient, $V_{\parallel T}=-1.17(1-0.67\varepsilon^{1/2})cT_i/(eB_pL_T)$, where L_T is the ion temperature gradient scale length and the coefficient $1.17(1-0.67\varepsilon^{1/2})$ is appropriate for the poloidal flow in the banana regime.[10] Assuming the current is inductively driven, ignoring bootstrap currents, the electric field is directly related to the parallel current $J_{\parallel}$ as evaluated in Appendix B and given by Eqs. (B7) and (B8)

$$\frac{V_{\parallel i}}{V_{\parallel T}}\approx 4.5(1+2.0\varepsilon^{1/2})\frac{L_T}{\beta_{pe}r}\left(\frac{mT_i}{MT_e}\right)^{1/2}\left(\frac{2\pi rJ_{\parallel}}{cB_p}\right), \tag{42}$$

where r is the minor radius. In writing Eq. (42) we have used $Z=1$, and kept $\varepsilon^{1/2}$ corrections to L, Eq. (B8), and Eq. (38) with the numerical values of $\langle\langle Q^p\rangle\rangle$ inserted. The coefficient of the $\varepsilon^{1/2}$ correction in Eqs. (39) and (42) is reduced by 0.6 if the full Hirshman–Sigmar result of Eq. (A13) is employed. Here the factor $2\pi rJ_{\parallel}/cB_p$ is a measure of the current density profile, equal to unity for uniform current. At the half-radius point L_T/r and T_i/T_e may typically also be approximately one. The quantity $\beta_{pe}=8\pi N_eT_e/B_p^2$, which is the poloidal beta accounting only for electron pressure, is typically about 0.25 in Alcator C-Mod cases. Taking $\varepsilon=1/3$, the combination of these factors is enough to counterbalance the mass ratio factor, leading to $V_{\parallel i}/V_{\parallel T}\sim0.6$ for deuterium. Thus, the inductive electric field velocity is comparable to the accepted neoclassical poloidal rotation term, and this is likely to be true in any tokamak with inductive current drive in the banana regime. The only situation in which the temperature gradient term is likely to be completely dominant is in extremely high poloidal beta plasmas, or in transport barriers where $L_T\ll r$.

Although the effect we have calculated is of comparable magnitude to the experimentally observed toroidal flow, and in the same direction (co-current), it does not represent a source or transport of toroidal momentum itself. Its main effect, therefore, is not to cause toroidal rotation but to change the relationship between the radial electric field and the toroidal velocity.[11] In other words, if $E_{\parallel}$ were turned off (which it could perhaps be by noninductive current drive), then the radial electric field would be forced to change if the toroidal (and hence parallel) velocity remained constant. In practice this means that the relationship between measurements of parallel velocity and radial electric field needs to be corrected for this parallel electric field effect on ion velocity.

An experimental test of the validity of the neoclassical theory, including this new term, requires a measurement of *poloidal* velocity, and specifically the velocity of the bulk ions. There do not seem to be sufficient experimental data yet to perform this detailed test, although considerable information is available on impurity velocities in the Tokamak Fusion Test Reactor (TFTR) (see the Appendix of Ref. 12) and the DIII-D tokamak.[13] Electrostatic potential measurements were performed in the Texas Experimental Tokamak (TEXT),[14] but in the plateau regime where the 1.17 in the temperature gradient coefficient must be replaced by -0.5 and where we expect the inductive velocity to be substantially smaller because the trapped particles are collisional and reduce E_* below the banana level.

V. CONCLUSIONS

We have evaluated the effect of the inductive electric field of a tokamak on the parallel ion flow in the banana regime and demonstrated that it is surprisingly large and quantitatively important. Moreover, we have shown that the parallel ion flow that arises in a torus in response to $E_{\parallel}$ does not vanish in the limit of small inverse aspect ratio, $\varepsilon\ll1$. As so often is the case in neoclassical theory, $\varepsilon\to0$ is a singular limit. Prior neoclassical treatments have invariably neglected the response of the ions to the inductive electric field and thereby ignored its effect on the poloidal ion flow. This weak coupling assumption is thought to be valid for evaluating transport coefficients,[2] but our results lead us to conclude that it is not well satisfied for evaluating the poloidal ion flow. As a result, the inductive electric field modification to the poloidal ion flow that we evaluate here should be added to the usual banana regime ion temperature gradient drive.

ACKNOWLEDGMENTS

This work was supported by U.S. Department of Energy Grant Nos. DE-FG02-91ER-54109 and DE-FC02-99ER54512 at the Plasma Science and Fusion Center of the Massachusetts Institute of Technology, and was jointly funded by the U.K. Department of Trade and Industry, and Euratom.

APPENDIX A: IMPROVED ION–ION TREATMENTS

The model collision operator, Eq. (8), used in the main text is a convenient operator, with appropriate conservation properties.[6,7] It permits a complete analytic solution of the bounce averaged ion kinetic equation, Eq. (7). This model operator describes pitch angle scattering with the correct collisional rate v, but it replaces the rest of the Fokker–Planck operator by a simple heuristic momentum conserving term. Hirshman and Sigmar[8] have, however, improved on this model and developed a systematic approach to generating similar approximations to the Fokker–Planck collision operator. Their operators take account of the differing rates for pitch angle scattering, slowing down, energy diffusion, etc. For linear problems in which the drive in the kinetic equation is odd in $v_\parallel$, their operators are also relatively simple and reduce the solution of Eq. (7) to a simple linear algebra problem of modest dimensions. Applied to the classical Spitzer problem,[2,9] the Hirshman–Sigmar operator, which we will use in this appendix, has been shown to be accurate to better than 1%.[8] It has also been shown to give accurate results for neoclassical resistivity in the large aspect ratio limit ($\varepsilon \to 0$). Since its derivation is independent of any geometrical simplifications, its use in neoclassical problems is not restricted to the large aspect ratio limit, and there is reason to expect that it will also yield accurate results at finite aspect ratio.

The operator consists of a Lorentz, pitch angle scattering, part, together with four separate momentum conserving contributions

$$C_{ii}\{f_{1i}\}=\nu v_\parallel \frac{\partial}{\partial\mu}\left(\frac{\mu v_\parallel}{B}\frac{\partial f_{1i}}{\partial\mu}\right)+\frac{M}{T_i}v_\parallel f_{0i}\left[(\nu-\nu_s)\frac{u(x)}{2x^2}+s\nu_s+x^2(h\nu_h+k\nu_k)\right], \tag{A1}$$

where $x=(Mv^2/2T_i)^{1/2}$. In Eq. (A1) the frequencies ν_j are functions of energy, and $u(x)$, r, h, and k are velocity space moments of f_{1i} defined as follows:

$$\nu(x)=\nu_{ii}[\Phi(x)-G(x)]/x^3,\quad \nu_s=4\nu_{ii}G(x)/x,$$
$$\nu_h=3\nu_{ii}[3G(x)+4x^2G(x)-2\Phi(x)]/x^3,$$
$$\nu_k=2\nu_{ii}[2G(x)-4x^2G(x)+\Phi(x)]/x^3, \tag{A2}$$
$$\Phi(x)=Erf(x),\quad G(x)=[\Phi(x)-x\Phi'(x)]/2x^2$$

and

$$u(x)=\frac{3}{4\pi}\int d\Omega v_\parallel\frac{f_{1i}}{f_{0i}},\quad s=\frac{3\int d^3v v_\parallel \nu_s f_{1i}}{2\int d^3v x^2\nu_s f_{0i}},$$
$$h=\frac{3\int d^3v v_\parallel \nu_h x^2 f_{1i}}{2\int d^3v x^6\nu_h f_{0i}},\quad k=\frac{3\int d^3v v_\parallel \nu_k x^2 f_{1i}}{2\int d^3v x^6\nu_k f_{0i}}, \tag{A3}$$

with $d\Omega$ the incremental velocity space solid angle and ν_{ii} defined following Eq. (9).

The method of solution of Eq. (7), using this collision operator, is analogous to that outlined in the main text. The equation is integrated once in the pitch angle variable μ to obtain an expression for $\partial f_{1i}/\partial\mu$, which still contains the moments $u(x)$, s, h, and k. This expression is then used to generate four equations for these moments, which are calculated explicitly, thus completing the solution for f_{1i}. Finally the longitudinal ion flow is obtained from Eq. (17). However, whereas the integral term Y of the simple model operator can be obtained analytically as a function of the effective passing particle fraction I [see Eq. (14)], closed analytic forms for $u(x,I)$, $s(I)$, $h(I)$, and $k(I)$ cannot be obtained from the Hirshman–Sigmar operator. The added complexity is caused by the appearance of the energy dependent moment $u(x,I)$, which must be eliminated separately from the s, h, and k moments, and results in the appearance of I dependent integrals as will be shown shortly [see Eqs.(A7) and (A8)]. Numerical evaluation of these integrals is required for each I value, and the resulting ion longitudinal flow can then be fitted by a low order polynomial in I.

The solution proceeds as follows. Integrating the ion kinetic equation once yields

$$\frac{\partial f_{1i}|_p}{\partial\mu}=-\frac{f_{0i}X(x)}{\nu\langle v_\parallel\rangle} \tag{A4}$$

for passing ions, and zero for trapped ions, where

$$X(x)=\left\langle\frac{eBE_*}{M}\right\rangle+\frac{(\nu-\nu_s)}{2x^2}\langle Bu(x)\rangle+\nu_s\langle Bs\rangle+x^2(\nu_h\langle Bh\rangle+\nu_k\langle Bk\rangle). \tag{A5}$$

Using this expression for $\partial f_{1i}/\partial\mu$ the moments $\langle Bu(x)\rangle$, $\langle Bs\rangle$, $\langle Bh\rangle$, and $\langle Bk\rangle$ can be evaluated. After elimination of $\langle Bu(x)\rangle$ the equations for $\langle Bs\rangle$, $\langle Bh\rangle$, and $\langle Bk\rangle$ take the form

$$\langle Bs\rangle[\alpha_{4s}-I\beta_{4ss}]=I[\langle eBE_*/M\rangle\beta_{4s}+\langle Bh\rangle\beta_{6sh}+\langle Bk\rangle\beta_{6sk}],$$
$$\langle Bh\rangle[\alpha_{8h}-I\beta_{8hh}]=I[\langle eBE_*/M\rangle\beta_{6h}+\langle Bs\rangle\beta_{6sh}+\langle Bk\rangle\beta_{8hk}], \tag{A6}$$
$$\langle Bk\rangle[\alpha_{8k}-I\beta_{8kk}]=I[\langle eBE_*/M\rangle\beta_{6k}+\langle Bs\rangle\beta_{6sk}+\langle Bh\rangle\beta_{8hk}],$$

with

$$\alpha_{nj}=\frac{2}{\sqrt{\pi}}\int_0^\infty dx e^{-x^2}x^n\nu_j,$$

$$\beta_{nj}=\frac{2}{\sqrt{\pi}}\int_0^\infty \frac{dx e^{-x^2}x^n \nu_j}{(1-I)\nu+I\nu_s}, \tag{A7}$$

$$\beta_{nij}=\frac{2}{\sqrt{\pi}}\int_0^\infty \frac{dx e^{-x^2}x^n \nu_i\nu_j}{(1-I)\nu+I\nu_s}.$$

Using Eqs. (A4) and (A5) the parallel ion flow velocity can also be obtained in terms of $\langle eBE_*/M\rangle$ and the moments $\langle Bu(x)\rangle$, $\langle Bs\rangle$, $\langle Bh\rangle$, and $\langle Bk\rangle$. Eliminating $\langle Bu(x)\rangle$ from this expression gives

$$\frac{V_{\parallel i}}{B}=\frac{4I}{3\langle B^2\rangle}(\langle eBE_*/M\rangle\beta_4+\langle Bs\rangle\beta_{4s}+\langle Bh\rangle\beta_{6h} +\langle Bk\rangle\beta_{6k}). \tag{A8}$$

Finally, solving the 3×3 matrix problem for $\langle Bs\rangle$, $\langle Bh\rangle$, and $\langle Bk\rangle$ and substituting the results into the preceding expression for $V_{\parallel i}$ we obtain an expression for the ion flow as a function of $\langle BE_*\rangle/\nu_{ii}$ and I, the fraction of passing ions. Using the lowest order Hirshman–Sigmar approximation, which retains only the $u(x)$ and s momentum conserving terms $(h=0=k)$, the result is

$$\frac{V_{\parallel i}}{B}=\frac{4eI\langle BE_*\rangle}{3M\langle B^2\rangle}\left(\beta_4+\frac{I\beta_{4s}^2}{\alpha_{4s}-I\beta_{4ss}}\right), \tag{A9}$$

while a more complicated expression is obtained when the full Hirshman–Sigmar operator is used. In the above expression all the β coefficients are functions of the circulating particle fraction I and must be calculated numerically. The α coefficients are numerical. The normalized ion flow

$$\bar{V}(I)=\frac{V_{\parallel i}}{B}\frac{M\nu_{ii}\langle B^2\rangle(1-I)}{e\langle E_*B\rangle} \tag{A10}$$

has been calculated over the complete range $0<I<1$, for both the lowest order Hirshman–Sigmar operator and the full Hirshman–Sigmar operator. The results are shown in Fig. 1, together with the analytic expression obtained in the main text using the simple deflection operator of Eq. (8). Simple analytic fits to these results are as follows:

$$\bar{V}=I[2.5I+5.4(1-I)], \tag{A11}$$

$$\bar{V}_{hs0}=I[5.05-3.08I+0.53I^2], \tag{A12}$$

and

$$\bar{V}_{hs}=I[4.74-3.01I+0.78I^2]. \tag{A13}$$

APPENDIX B: ELECTRON–ELECTRON COLLISIONS

To retain electron–electron collisions to evaluate the relation between $\langle BE_*\rangle$ and $\langle BE_\parallel\rangle$ we use the model operator of Eqs. (8) and (9) to determine the passing response by solving

$$\left\langle \frac{B}{v_\parallel}[C_{ee}\{f_{1e}|_p\}+L_{ei}\{f_{1e}|_p\}\right\rangle=\frac{e}{T_e}\langle BE_\parallel\rangle f_{0e}. \tag{B1}$$

Integrating once and proceeding as in Sec. II gives

$$\frac{\partial f_{1e}|_p}{\partial\mu}=\frac{e\langle BE_\parallel\rangle Q_Z f_{0e}}{T_e\nu_{ee}Q\langle v_\parallel\rangle}\left[1+\frac{IQ\langle\langle Q_Z\rangle\rangle}{\langle\langle Q\rangle\rangle-I\langle\langle QQ_Z\rangle\rangle}\right], \tag{B2}$$

where Q is defined in Eq. (9) and $Q_Z=Q/[Q+(Z/x^3)]$ with $x=(mv^2/2T_e)^{1/2}$ for electrons. Solving Eq. (22) for the Spitzer function using the same model electron–electron operator gives

$$f_{1s}=-\frac{eE_\parallel v_\parallel Q_Z f_{0e}}{T_e\nu_{ee}Q}\left[1+\frac{Q\langle\langle Q_Z\rangle\rangle}{\langle\langle Q\rangle\rangle-\langle\langle QQ_Z\rangle\rangle}\right]. \tag{B3}$$

Inserting Eqs. (28), (B2), and (B3) into Eq. (24) with the parallel ion flow term neglected, performing the integrals, and multiplying by B and flux surface averaging gives Eq. (33).

To form the parallel friction we first integrate Eq. (3) by parts and recall Eq. (28) to obtain

$$F_{\parallel ei}=m\int d^3v\,\nu_{ei}v_\parallel\mu\partial f_{1e}/\partial\mu|_p. \tag{B4}$$

Inserting Eq. (B2), multiplying by B, flux surface averaging, performing the integrals by employing Eqs. (15) and (19) gives

$$F_{\parallel ei}=eN_e\langle BE_\parallel\rangle I\left\langle\left\langle\frac{ZQ_Z}{x^3Q}\left[1+\frac{IQ\langle\langle Q_Z\rangle\rangle}{\langle\langle Q\rangle\rangle-I\langle\langle QQ_Z\rangle\rangle}\right]\right\rangle\right\rangle. \tag{B5}$$

Forming $\langle BE_*\rangle$ by using $ZQ_Z/x^3Q=1-Q_Z$ to rearrange terms yields Eq. (35).

Using Eq. (B2) to evaluate the parallel current

$$J_\parallel=-e\int d^3v\,v_\parallel f_{1e}=e\int d^3v\,v_\parallel\mu\partial f_{1e}/\partial\mu|_p, \tag{B6}$$

gives

$$J_\parallel=\frac{e^2N_e\langle BE_\parallel\rangle BI}{m\nu_{ee}\langle B^2\rangle}\left\langle\left\langle\frac{Q_Z}{Q}\left[1+\frac{IQ\langle\langle Q_Z\rangle\rangle}{\langle\langle Q\rangle\rangle-I\langle\langle QQ_Z\rangle\rangle}\right]\right\rangle\right\rangle. \tag{B7}$$

At large aspect ratio and for $Z=1$

$$I\left\langle\left\langle\frac{Q_Z}{Q}\left[1+\frac{IQ\langle\langle Q_Z\rangle\rangle}{\langle\langle Q\rangle\rangle-I\langle\langle QQ_Z\rangle\rangle}\right]\right\rangle\right\rangle\approx2.45I\left(\frac{1-0.186I}{1-0.373I}\right), \tag{B8}$$

which becomes $3.2(1-2.0\varepsilon^{1/2})$ at large aspect ratio.

[1] I. H. Hutchinson, J. E. Rice, R. S. Granetz, and J. A. Snipes, Phys. Rev. Lett. **84**, 3330 (2000).
[2] F. L. Hinton and R. D. Hazeltine, Rev. Mod. Phys. **48**, 239 (1976).
[3] S. P. Hirshman and D. J. Sigmar, Nucl. Fusion **21**, 1079 (1981).
[4] A. A. Ware, Phys. Rev. Lett. **25**, 15 (1970).
[5] A. A. Galeev, Sov. Phys. JETP **32**, 752 (1971).
[6] M. N. Rosenbluth, R. D. Hazeltine, and F. L. Hinton, Phys. Fluids **15**, 116 (1972).
[7] J. W. Connor, R. C. Grimm, R. J. Hastie, and P. M. Keeping, Nucl. Fusion **13**, 211 (1973).
[8] S. P. Hirshman and D. J. Sigmar, Phys. Fluids **19**, 1532 (1976).
[9] L. Spitzer, Jr., *Physics of Fully Ionized Gases* (Wiley, New York, 1962).
[10] S. P. Hirshman, Phys. Fluids **31**, 3150 (1988).
[11] M. N. Rosenbluth, P. H. Rutherford, J. B. Taylor, E. A. Frieman, and L. M. Kovrizhnikh, in *Plasma Physics and Controlled Nuclear Fusion Research* (International Atomic Energy Agency, Vienna, 1971), Vol. I, p. 495.

[12]D. R. Ernst, R. E. Bell, M. G. Bell, R. V. Budny, B. Coppi, G. W. Hammett, R. J. Hawryluk, K. W. Hill, D. K. Mansfield, D. R. Mikkelsen, H. K. Park, M. Porkolab, S. D. Scott, G. L. Schmidt, E. J. Synakowski, M. C. Zarnsdorff, and the TFTR Group, Phys. Plasmas **7**, 615 (2000).

[13]J. Kim, K. H. Burrell, P. Gohil, R. J. Groebner, F. L. Hinton, Y. B. Kim, W. Mandl, R. Seraydarian, and M. R. Wade, Plasma Phys. Controlled Fusion **36**, A183 (1994).

[14]X. Z. Yang, B. Z. Zhang, A. J. Wooton, P. M. Schoch, B. Richards, D. Baldwin, D. L. Brower, G. G. Castle, R. D. Hazeltine, J. W. Heard, R. L. Hickok, W. L. Li, S. C. McCool, V. J. Simcic, Ch. P. Ritz, and C. X. Yu, Phys. Fluids B **3**, 3448 (1991).